DOI: 10.61782/fa.2023.0022

forum acusticum 2023

A LOW COMPUTATIONAL COMPLEXITY LOCAL ACTIVE NOISE CONTROL SYSTEM FOR ADJACENT AIRCRAFT SEATS

Dimitrios Mylonas[1*] **Alberto Erspamer**[1] **Christos Yiakopoulos**[1]
Ioannis Antoniadis[1]
[1] School of Mechanical Engineering, National Technical University of Athens, Greece

ABSTRACT

The excessive Sound Pressure Level at the interior of aircrafts can create very annoying flight conditions for the passengers, as it can reach 90 dB-95 dB for some aircraft types (e.g. tilt rotors). These acoustic disturbances, which have low frequency components, can be successfully attenuated by Active Noise Control systems installed in the seat headrests. The present work proposes a system based on mixed error FxLMS algorithm because of its low complexity and robustness. It is also responsible for the mitigation of the acoustic pressure around the headrests of two adjacent seats, in order to save computational resources and hardware. 3D simulations with Finite Element Method and experiments in a cabin mock-up have shown that the proposed system provides a 10 dB quiet zone for a synthetic acoustic disturbance. It is also demonstrated that the size of the quiet zone allows gentle head movements while using a small number of microphones and loudspeakers.

Keywords: *noise canceling headrest, aircraft cabin, low frequency attenuation, mixed error FxLMS.*

1. INTRODUCTION

The mitigation of low frequency noise at the interior of an aircraft's cabin is a field where Active Noise Control (ANC) techniques can have a significant contribution. In propeller driven as well as in tilt rotor aircrafts, the noise spectra are dominated by harmonics of the Blade Passage Frequency (BPF) [1]. Especially in tilt rotors these harmonics, which are below 400 Hz lead to interior noise levels that can be higher than conventional helicopters [2]. Although the traditional approach to active noise control in vehicles is to attenuate acoustic disturbances on a global scale, recent studies have focused on local ANC around the seat's headrest [3,4]. These systems try to create quite zones around the passengers' ears so as to allow gentle head movement.

The extent of the generated quiet zone, as well as the complexity of the control algorithm, provide significant challenges. Using multiple microphones and loudspeakers combined with a Multiple Input-Multiple Output (MIMO) adaptive control algorithm (e.g. FxLMS) is a well-known strategy for achieving noise attenuation in a large area. Several studies proposed effective methods for improving this strategy, such as modifying the control algorithm [5] or experimenting with the location and the number of secondary sources [6,7].

However, these systems are often characterized by high computational complexity and large number of transducers, especially when each system is dedicated to a single seat. In an attempt to develop a computationally efficient and practically feasible ANC headrest, the current study investigates a system based on a simplified mixed error FxLMS algorithm [8]. In addition, this system aims to attenuate the acoustic pressure around the headrests of two adjacent seats instead of one, in order to save computational resources and hardware. Furthermore, the placement of the error microphones over a wide area, as well as the use of subwoofers with larger diameters than standard loudspeakers, contribute to the expansion of the quiet zone.

The paper is structured as follows. In section 2, the

*__Corresponding author__: dimimyl579@mail.ntua.gr.

system's setup is presented along with the control algorithm. In section 3, the ANC headrest is analyzed through FEM simulations, while in section 4 it is evaluated experimentally in an aircraft's cabin mockup. Finally, in sections 5 and 6, there is a discussion of the results and conclusions emerged from this work.

2. METHOD

The ANC system that aims to create a quiet zone in front of two adjacent airplane seats consists of two secondary sources (subwoofers) and three microphones (Fig. 1).

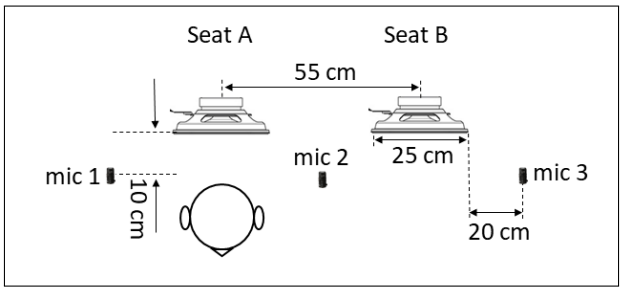

Figure 1: The ANC setup for two adjacent seats that consists of two subwoofers and three microphones.

The driving signal (anti-noise signal), which is the same for the two secondary sources derives from Eqn. (1). In the following equations, the vectors are denoted by bold letters.

$$y(n) = \mathbf{w}^T(n)\mathbf{x}(n) \tag{1}$$

where x is the reference signal obtained by a sensor close to the noise source, w is a vector of adaptive filter coefficients computed by Eqn. (2).

$$\mathbf{w}(n) = [w_1(n)\, w_2(n)\, w_3(n) \ldots w_L(n)] \tag{2}$$

where L is the filter length.

The mixed error FxLMS algorithm is used to compute **w**, because of its low computational complexity. The cost function that has to be minimized is the instantaneous squared sum of the three error signals given by Eqn. (3).

$$J(n) = [e_1(n) + e_2(n) + e_3(n)]^2 = e_{mix}^2 \tag{3}$$

The gradient of the cost function is given by equation Eqn. (4)

$$\nabla J(n) = 2[\nabla e_{mix}(n)]e_{mix}(n) \tag{4}$$

In addition, the error signal of each microphone is given by Eqn. (5).

$$e_i(n) = d_i(n) + \mathbf{s}_i(n) * [\mathbf{w}^T(n)\mathbf{x}(n)], \quad i = 1, 2, 3. \tag{5}$$

where d_i and $\mathbf{s}_i$ are the acoustic disturbance and the secondary path at the i^{th} microphone respectively and * denotes the convolution operator.

Then we can extract the gradient of the mixed error by Eqn. (6).

$$\begin{aligned} &\nabla e_{mix}(n) = [\mathbf{s}_1(n) + \mathbf{s}_2(n) + \mathbf{s}_3(n)] * \mathbf{x}(n) \Rightarrow \\ &\nabla e_{mix}(n) = \mathbf{s}(n) * \mathbf{x}(n) = \mathbf{x}'(n) \end{aligned} \tag{6}$$

where **s**(n) is the parallel combination of the secondary paths of the three error microphones, which is computed during a preliminary identification stage. During this process, Least Means Square (LMS) algorithm was used. Both secondary sources were driven by white noise, which was the reference signal for the LMS. The error signal was the sum of the signals captured by the three microphones.

Finally, the coefficients of **w** are derived from Eqn. (7) by combining Eqn. (4) and Eqn. (6).

$$\begin{aligned} &\mathbf{w}(n+1) = \mathbf{w}(n) - \frac{\mu}{2}\nabla J(n) \Rightarrow \\ &\mathbf{w}(n+1) = \mathbf{w}(n) + \mu\mathbf{x}'(n)e_{mix}(n) \end{aligned} \tag{7}$$

where μ is the step size of the minimization process.

At this point, it is important to note that the suggested algorithm, which is an alternative to the classic Multiple Input Multiple Output (MIMO) FxLMS algorithm [9], can converge to the MIMO FxLMS solution when the three error signals are almost identical [8]. This could happen when they are placed to a very close distance, which is not effective in the current headrest application because the size of the quiet zone would be reduced. Although the error microphones are not close to one another, the proposed methodology achieves a significant attenuation of the acoustic pressure over a large area, as demonstrated in Sec. 3 and Sec. 4 .

3. SIMULATION RESULTS

The three dimensional simulations of the proposed ANC headrest were conducted using time domain Finite Element Method in Comsol Multiphysics®. The cabin mockup of the aircraft was designed to be identical to the

one installed in the laboratory for the system's experimental testing Sec. 4. The dimensions of the cabin are 3m along the x axis, 2.45m along the y axis, and 2m along the z axis, where the axis refer to Fig. 2. Moreover, the cabin's

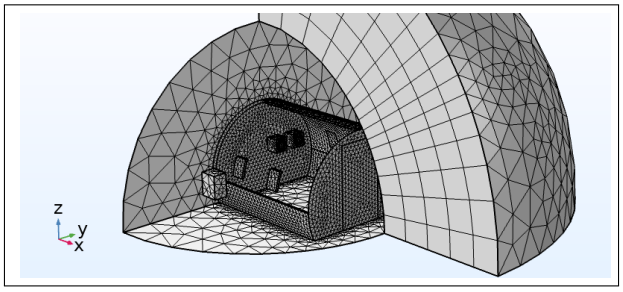

Figure 2: Mesh of the cabin model and the spherical PML which simulates free space.

walls were modeled as absorbing boundaries, in order to allow the acoustic disturbance produced by an external noise source to enter the cabin. Finally, a semi-spherical Perfectly Matched Layer (PML) was placed around the cabin in order to model free space. The meshing of the model is also demonstrated in Fig. 2. The driving signal of the secondary sources presented in Sec. 2 was inserted into the model by adding global equations, which control the normal acceleration of the boundaries that model the diaphragms of the subwoofers (Fig. 3). A loudspeaker that was placed one meter away from the cabin was used as the noise source. It was driven by a synthetic signal consisting of three 24 Hz BPF harmonics at 72 Hz, 96 Hz, and 120 Hz.

The attenuation of the Sound Pressure Level (SPL) reached 18 dB in front of seat A and 20 dB in front of seat B. In addition, the maximum attenuation was achieved

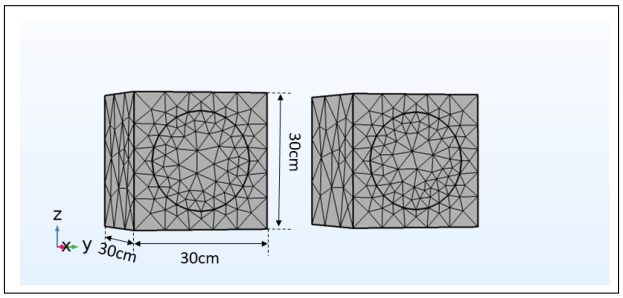

Figure 3: Mesh and dimensions of the secondary sources used in the FEM model.

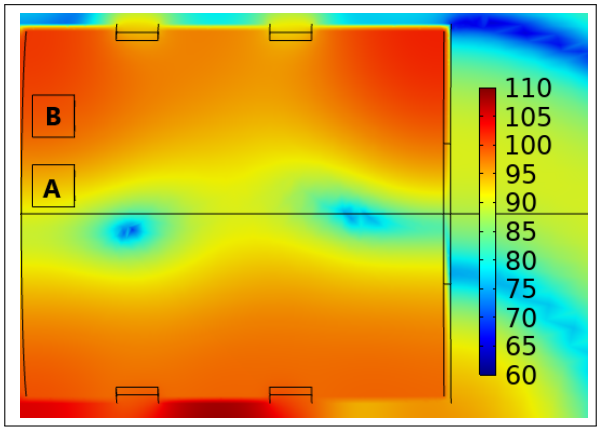

(a)

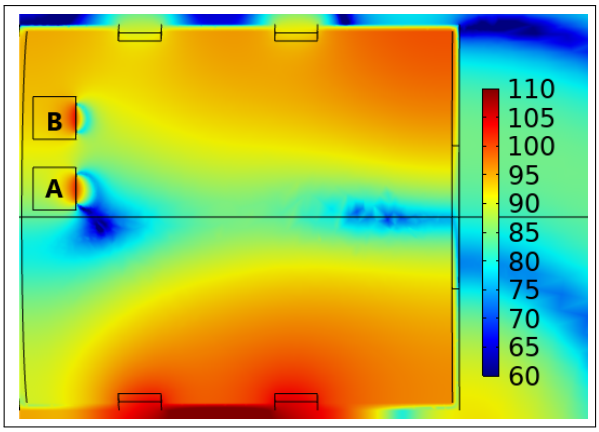

(b)

Figure 4: Top view of the cabin mockup modeled using FEM (a) before and (b) after the activation of the ANC system.

10 cm to 15 cm far from the surface of the subwoofers Fig. 4b.The quiet zone had a surface area of $30cm \times 30cm$ in front of both seats as well as over the area between them. Furthermore, the rest of the cabin was not negatively affected by the system's activation. Instead, the acoustic pressure was reduced in the vicinity of the subwoofers. At this point we have to mention that the results refer to the plane along the z axis with height 120 cm, which coincides with the z coordinate of the center of the subwoofers. Similar results were obtained for heights between 105 cm and 135 cm. As a result, the generated quiet zone is adequate for gentle head movements by passengers of various heights.

4. EXPERIMENTAL EVALUATION

The experimental setup consists of two Pioneer TS-A250S4 subwoofers to reproduce the low frequencies required by the application and three Shure MX 183 microphones Fig. 4b. The control algorithm was implemented in National Instruments CRIO-9030 microcontroller. More specifically the FPGA part (Xilinx Kintex-7) was used in order take advantage of its parallel data processing capability along with Labview® platform.

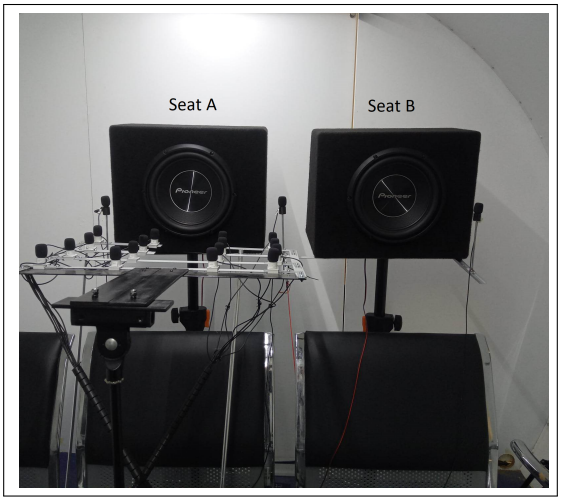

Figure 5: The ANC system for two adjacent seats installed in the cabin mockup.

The acoustic disturbance was similar to the one used in the FEM simulation, with three sinusoidal components at 72 Hz, 96 Hz, and 120 Hz, as well as low-amplitude white noise. It was reproduced by a noise source located adjacent to the cabin mockup. A microphone located 5 cm away from the noise source was also used to capture the reference signal. Finally, a grid of 16 microphones covering an area of $30cm \times 25cm$ was used to measure the acoustic pressure in front of the two seats. Linear interpolation was also used to estimate the acoustic pressure between the measurement points.

For both seats, the maximum SPL attenuation was achieved 10 cm away from the error microphones, which coincides with the simulation results. It reached 15.5 dB in front of seat A (6a), and 13 dB in front of seat B (6b). However, the surface of the zone where this attenuation was maintained differed between the two headrests. At seat A there is a quiet zone which is 20 cm wider than seat B. Although the highest SPL attenuation is not achieved in a large quiet zone in the case of seat B, the amplitude of the 72 Hz and 96 Hz harmonics is reduced by more than 10 dB for all measurement points Tab. 1. However, efficient reduction in some areas is not achieved in the case of the 120 HZ harmonic, resulting in a decline in system's performance around microphone D. Finally, for the four measuring microphones, the average attenuation was greater for the 96 Hz harmonic, reaching 18.25 Hz, and smaller for the 20 Hz harmonic, reaching 8.25 Hz.

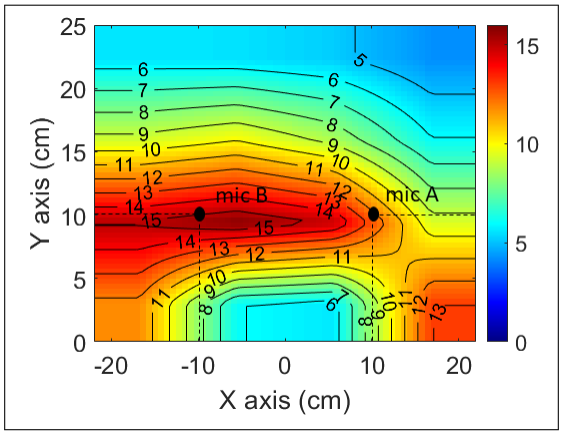

(a)

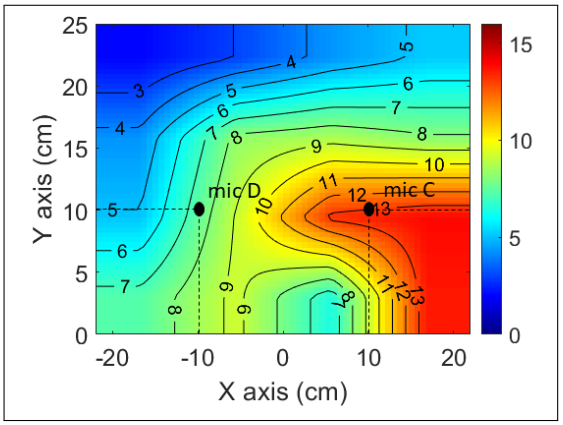

(b)

Figure 6: Attenuation of the Sound Pressure Level in front of a) seat A and b) seat B. The error microphones are located at the zero level of the y axis. Measurement microphones A and C correspond to the passenger's right ear, while microphones B and D to passenger's left ear.

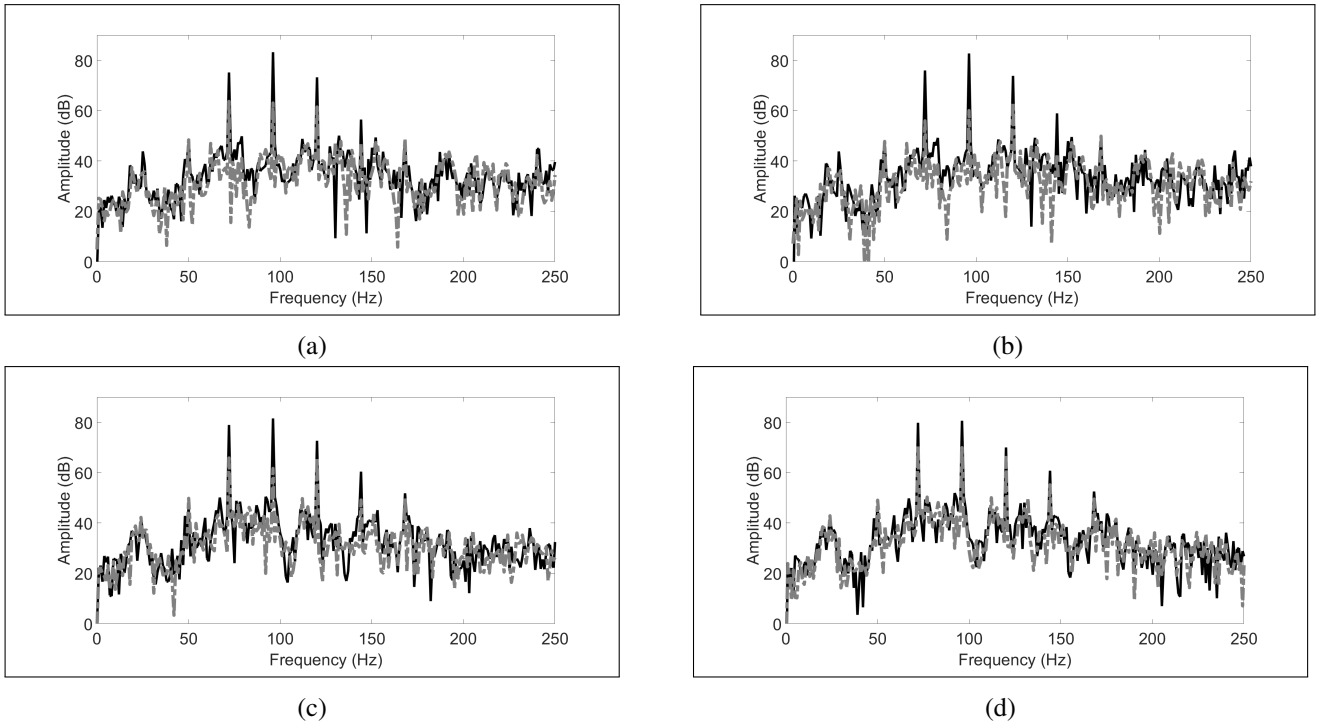

Figure 7: Frequency spectrums captured by a) microphone A, b) microphone B, c) microphone C and d) microphone D demonstrated in Figs. 6a and 6b before (black line) and after (grey dotted line) the ANC activation.

5. DISCUSSION

The mixed-error solution given by Eqn. (7) can converge to the one derived from conventional multichannel FxLMS, if the outputs of each error microphone are almost identical. This hypothesis is not valid in the case of the current headrest application. However, the proposed system achieves significant acoustic pressure attenuation through an area around the central error microphone. As we move closer to the edge error microphones, the attenuation decreases. This behaviour is further explained in Appendix.

Furthermore, the 10 dB quiet zone is extended 10 cm - 15 cm away from the error microphones, along the y axis. This is due to the distance between the subwoofers' diaphragms and the error microphones (10 cm), as the radial extent of 10 dB quiet zone depends on the distance from secondary sources to cancelling microphones [10]. In addition, the size of the quiet zone depends on the diameter of the subwoofers' diaphragm. This is another contribution of the subwoofers aside from the mitigation of low frequency harmonics.

Finally, the proposed system exhibits the behavior described in the previous paragraphs for low frequency acoustic disturbances, when the wavelength is bigger than the distance between the error microphones. For this reason it is suitable for the specific application where acoustic disturbances due to aircraft rotors or propellers include frequencies below 400 Hz.

6. CONCLUSION

This paper presents an Active Noise Control system that that aims to mitigate acoustic pressure around the headrests of two adjacent aircraft seats. It is based on an alternative to the original multichannel FxLMS algorithm, which has a lower computational complexity. The system was evaluated using three-dimensional FEM simulations and experiments in an aircraft's cabin mockup, which demonstrated that the aforementioned mixed error FxLMS can be used for an ANC headrest application, achieving a more than 10 dB attenuation of the sound pressure level over a large area around the passenger's ears. The placement of the error microphones at the edges of

Frequency (Hz)	SPL Attenuation (dB)				
	micA	micB	micC	micD	Average
72	12	20	13	9	13.5
96	20	22	20	11	18.25
120	12	10	7	4	8.25

Table 1: Attenuation of three BPF harmonics' amplitudes after the activation of the proposed ANC system.

the seat headrests, as well as the large diameter of the secondary sources, contributed to the expansion of the quiet zone. Finally, the proposed system is a promising solution for real-world applications due to the limitations of the convolution operations needed comparing to the original multichannel algorithm, as well as the coverage of two seats by only two secondary sources.

7. APPENDIX

The cost function of Eqn. (3) can be written as follows:

$$J(n) = \underbrace{e_1^2(n) + e_2^2(n) + e_3^2(n)}_{J_1(n)} + ... \\ ... + \underbrace{2e_1(n)e_2(n) + 2e_2(n)e_3(n) + 2e_1(n)e_3(n)}_{J_2(n)} \quad (8)$$

Thus, the gradient of the cost function is:

$$\nabla J(n) = \nabla J_1(n) + \nabla J_2(n) \quad (9)$$

In addition, at low frequencies, when the distance between the microphones is much less than the wavelength, the acoustic pressure at the midpoint between microphones 1 and 2 can be estimated by Eqn. (10) [11].

$$e_{mid_{12}}(n) = \frac{e_1(n) + e_2(n)}{2} \quad (10)$$

Similar equations can be also written for the rest microphone couples. Furthermore, if the sum of the squares of the acoustic pressures is minimized, the potential acoustic energy is minimized [12]. Eqn. (12) gives the cost function for minimizing potential energy at the midpoints.

$$J_{mid}(n) = e_{mid_{12}}^2(n) + e_{mid_{13}}^2(n) + e_{mid_{23}}^2(n) = \\ = e_1^2(n) + e_2^2(n) + e_3^2(n) + ... \\ ...e_1(n)e_2(n) + e_2(n)e_3(n) + e_1(n)e_3(n) \quad (11)$$

Combining Eqn. (9) with Eqn. (11) we obtain:

$$J_{mid}(n) = J_1(n) + \frac{1}{2}J_2(n) \quad (12)$$

and

$$\nabla J_{mid}(n) = \nabla J_1(n) + \frac{1}{2}\nabla J_2(n) \quad (13)$$

As a result, the update equations for both cost functions are nearly similar, with the exception of a constant factor that only affects the convergence rate. The proposed methodology, therefore minimizes the acoustic energy at the midpoints between the three microphone pairs, which can explain the shape of the quiet zone presented in Fig. 6a and Fig. 6b.

8. ACKNOWLEDGEMENTS

The present work has been carried out in the framework of the PIANO project (Path Identification for Active Noise Control), funded by EU Horizon 2020 and Clean Sky JU under the Grant Agreement no. 885976.

9. REFERENCES

[1] S. Johansson and I. Claesson, "Active noise control in propeller aircraft," in *Proc. Conference for the Promotion of Research in IT at New Universities and at University Colleges in Sweden*, (Ronneby, Sweden), 2001.

[2] J. Ma, Y. Lu, X. Xu, and H. Yue, "Research on near field aeroacoustics suppression of tilt-rotor aircraft based on rotor phase control," *Applied Acoustics*, vol. 186, p. 108451, 2022.

[3] C.-Y. Chang, C.-T. Chuang, S. M. Kuo, and C.-H. Lin, "Multi-functional active noise control system on headrest of airplane seat," *Mechanical Systems and Signal Processing*, vol. 167, p. 108552, 2022.

[4] R. Han, M. Wu, C. Gong, S. Jia, T. Han, H. Sun, and J. Yang, "Combination of robust algorithm and head-tracking for a feedforward active headrest," *Applied Sciences*, vol. 9, no. 9, 2019.

[5] D. Shi, B. Lam, S. Wen, and W.-S. Gan, "Multichannel active noise control with spatial derivative constraints to enlarge the quiet zone," in *ICASSP 2020 - 2020 IEEE International Conference on Acoustics, Speech and Signal Processing (ICASSP)*, pp. 8419–8423, 2020.

[6] H. Sun, T. D. Abhayapala, and P. N. Samarasinghe, "A realistic multiple circular array system for active noise control over 3d space," *IEEE/ACM Transactions on Audio, Speech, and Language Processing*, vol. 28, pp. 3041–3052, 2020.

[7] T. Peleg and B. Rafaely, "Investigation of spherical loudspeaker arrays for local active control of sound," *The Journal of the Acoustical Society of America*, vol. 130, pp. 1926–1935, 10 2011.

[8] T. Murao, C. Shi, W.-S. Gan, and M. Nishimura, "Mixed-error approach for multi-channel active noise control of open windows," *Applied Acoustics*, vol. 127, pp. 305–315, 2017.

[9] S. M. Kuo and D. R. MOrgan, *Active Noise Control Systems Algorithms and DSP implementations*. New York: John Wiley and Sons Inc., 1996.

[10] P. Nelson and S. Elliot, *Active Control of Sound*. London: Academic Press Limited, 1992.

[11] H. Zhu, R. Rajamani, and K. A. Stelson, "Active control of acoustic reflection, absorption, and transmission using thin panel speakers," *The Journal of the Acoustical Society of America*, vol. 113, pp. 852–870, 01 2003.

[12] A. R. D. Curtis, P. A. Nelson, S. J. Elliott, and A. J. Bullmore, "Active suppression of acoustic resonance," *The Journal of the Acoustical Society of America*, vol. 81, pp. 624–631, 03 1987.